2. Phytoplankton; submitted by Christopher D. Hewes (Leg II), Roger Hewitt (Leg I), John Wieland (Leg II), B. Greg Mitchell (SIO) and Osmund Holm-Hansen (SIO).

2.1 Objectives: The overall objective of our research project was to assess the distribution and concentration of food reservoirs available to the herbivorous zooplankton populations throughout the AMLR study area during the austral summer. Specific objectives of our work included: (1) to determine the distribution and biomass of phytoplankton in the upper water column (surface to 750m), with emphasis on the upper 100m; (2) to measure pigment-specific absorption by total particulates, detritus and phytoplankton; (3) to measure the spectral attenuation of light with depth (4) to coordinate these activities with SeaWiFS satellite pass overs; (5) to calibrate satellite imagery of spectral reflectance to surface chlorophyll concentrations.

2.2 Methods and Accomplishments: The major types of data acquired during these studies are listed below, together with an explanation of the methodology employed.

(A) Sampling Strategy:

Protocols are to obtain water samples for analyses or to acquire data from various sensors are described below: (1) During Leg I, water samples were obtained from 10-liter Niskin bottles (with Teflon covered springs) which were closed at four standard depths (5, 30, 100, and 150m) from every upcast of the CTD/rosette unit. During Leg II, 5m samples were obtained from 10-liter Niskin bottles at all stations except for three stations in the Bransfield Strait where 9 depths (5, 10, 20, 30, 40, 50, 75, 100, and 150m) were sampled. Leg I occupied 41 stations and Leg II occupied 98 stations. These water samples were used for measurements described below. (2) During Leg II, two transmissometers (488 and 660nm wavelengths) were used to determine the attenuation of collimated light (by both scattering and absorption) during CTD-casts. The methodologies employed in our studies are described below. (3) For both legs, SeaWiFS satellite images were processed for monthly averaged chlorophyll concentration.

(B) Measurements and Data Acquired:

(1) Chlorophyll-*a* concentrations: Chl-*a* concentrations in the water samples (5, 30, 100, 150m Leg I; 5m Leg II except for three stations where profiles were obtained) from the Niskin bottles at every CTD station were determined by measurement of chl-*a* fluorescence after extraction in an organic solvent. Sample volumes of 100 - 250ml were filtered through glass fiber filters (Whatman GF/F, 25mm) at reduced pressure (maximal differential pressure of 1/3rd atmosphere). The filters with the particulate material were placed in 10ml of either 90% acetone (Leg I) or absolute methanol (Legs I and II) in 15ml tubes and the photosynthetic pigments allowed to extract at 4°C for at least 12 hours. The samples were then shaken, centrifuged, and the clear supernatant poured into cuvettes (13 x 100mm) for measurement of chl-*a* fluorescence before and after addition of two drops of 1.0 N HCl. Fluorescence was measured using two Turner Designs Fluorometers (model #10-005R for Leg I and model #700) both having been calibrated using spectrophotometrically determined chl-*a* concentrations of a prepared standard (Sigma). Stability of the fluorometers was verified daily by use of a fluorescence standard. Furthermore, 5m samples were also filtered onto glass fiber filters, wrapped in aluminum foil, and placed in liquid nitrogen until Leg II, at which time extraction in methanol (MeOH) and

analysis using the Turner Designs #700 was done. This allowed the different methods used for each leg to be compared.

(2) For 31 stations during Leg II, discrete samples were obtained between 1000 and 1600 GMT (corresponding with the SeaWiFS satellite pass over) for pigment analyses. Although water bottle samples obtained at 5m depth were the standard protocol, at 3 stations it was possible to obtain an additional 7 different depths (10, 20, 30, 40, 50, 75, 100m). For each analysis, except where noted 1-2 liters were filtered on 25mm Whatman GF/F filters.

- Particulate Absorption (a_p) and Soluble Absorption (a_s). Spectral absorption coefficients of particulate and soluble material were performed on a CARY 100 dual beam spectrophotometer.

- High Pressure Liquid Chromatography (HPLC). HPLC will be used for the analysis of (1) various chlorophylls and associated pigments, and (2) Microsporine-like Amino Acids (MAAs). Samples were frozen and stored in liquid nitrogen until their analyses can be made at SIO. Chlorophyll and associated pigments will be used to determine the proportions of algal classes contained in the phytoplankton community. MAAs absorb ultraviolet-B radiation and are thought to protect phytoplankton against photo-oxidative damage by UV damage to the photosystem.

- Particulate Organic Carbon and Nitrogen (POC/PON). Whatman GF/F filters used for sample preparation were combusted at 450°C prior to the cruise. Samples were frozen and will be analyzed by standard gas chromatography methods at the analytical facility at UC Santa Barbara.

- Phycoerythrins (PE). Cryptomonads are a common phytoflagellate in the AMLR study region and are distinguished from other phytoplankton in the area by PE. The filtered water samples were frozen and stored in liquid nitrogen until their analysis at SIO. PE will be measured using a Spex Fluoromax spectrofluorometer.

- Cell size spectrum. Two ml of water was frozen and stored in liquid nitrogen until analysis. A Coulter Epics flow-cytometer will be used to size cells and classify them in relation to chlorophyll and phycoerythrin fluorescence as well as forward light scatter.

(3) Measurement of beam attenuation: During Leg II, two single wavelength (488 and 660nm) C-star transmissometers (Wetlabs, Inc.) were placed on the Seabird Inc. CTD rosette for deployment at each station. Previous studies have shown that beam attenuation (660nm) coefficients can be used to estimate total particulate organic carbon in Antarctic waters (Villafañe *et al*., 1993). This calculation assumes that there is a negligible load of inorganic sediment in the water, a condition that is apparently satisfied throughout the study area.

(4) Corresponding approximately in time with the SeaWiFS satellite pass over (26 stations), a Satlantic free-fall SeaWiFS Profiling Multispectral Radiometer (SPMR) was deployed. The SPMR measured spectral downwelling irradiance and upwelling radiance at 13 wavelengths continuously from the surface to the bottom of the profile. Profile depths ranged from 50-150

meters depending on the station. Spectral values of normalized water-leaving radiance will be computed from the SPMR data and used to validate SeaWiFS data, as well as to develop Southern Ocean regional ocean color algorithms.

(5) SeaWiFS chlorophyll images were obtained for 8-day and monthly average composites from NASA archives. These data will be sufficient to evaluate the time-dependence and distribution of chl-*a* within our study region.

2.3 Results and Tentative Conclusions: An optical oceanography component was incorporated to the program this year (funds from NASA to Dr. Greg Mitchell, SIO), providing satellite (SeaWiFS) images of surface chlorophyll distributions, as well as *in-situ* light spectra profiling during Leg II and spectrophotometry of pigments.

(A) Although different methods for chlorophyll analysis were done for each Leg, the two yielded similar results (Figure 2.1). Phytoplankton biomass at 5m depth during Leg I averaged 1.17 ± 1.19 mg chl-*a* m^{-3}, and Leg II chl-*a* concentrations averaged 1.4 ± 1.1 mg m^{-3}. During Leg I, chl-*a* concentrations were estimated from discrete water samples and integrated over the upper 200m. Chl-*a* patterns followed hydrographic boundaries with highest values north of Southern Antarctic Circumpolar Current Front (SACCF). Lower values were observed to the south of the SACCF, increasing toward the southern boundary of the Antarctic Circumpolar Current. Integrated chl-*a* values were highest along the middle and northern portions of Transects SS05 and SS08 and lowest in the vicinity of the South Orkney Islands. During Leg II, the west section mean 5m chl-*a* was 0.95 ± 1.15 mg m^{-3}. This is higher than found for the mean of the same area in 1999, then having 0.6 ± 0.7 mg m^{-3}. Highest chl-*a* concentrations (3.0 - 4.7 mg m^{-3}) were found at the near coastal stations along King George Island, while lowest concentrations were found in the northern region of the survey (Type I waters, averaging 0.2 mg m^{-3}). Phytoplankton biomass measured for 5m samples in the Elephant Island area was 1.50 ± 1.07 mg chl-*a* m^{-3} (58 stations). These values compare to 1.64 ± 1.50 mg chl-*a* m^{-3} from Leg II of last year, and to the mean (1990-1999) February 5m values of 1.06 ± 1.23 mg chl-*a* m^{-3}. Therefore, although not the richest year observed, February 2000 had an above average phytoplankton crop in the Elephant Island sector. The highest value observed was 4.1 mg chl-*a* m^{-3} at Station A065 (just south of Elephant Island).

(B) Chl-*a* concentrations in the upper water column differ in various regions of the sampling grid as described in past reports. Since chl-*a* profiles were not possible at all stations this year, we can only present transmissometer data (Figure 2.3). Previously, stations with the lowest surface chl-*a* concentrations generally had a deep chl-*a* maximum at approximately 80m depth and are found in Drake Passage waters (e.g., Zone 1A water). Stations in the other water zones generally have higher chl-*a* values in the upper 20-30m of the water column, and no deep chl-*a* maximum. For the Drake Passage waters (Figure 2.3A), a small bulge in the C_t at the temperature minimum (arrow 1) corresponds with where the chl-*a* maximum is usually found. A maximum C_t was recorded near the base of the upper mixed layer (arrow 2). This maximum C_t was also observed at Station D104 (Figure 2.3B), and was a blend of Drake Passage and Bransfield Strait waters (e.g., Zone 1B water). Bransfield Strait water (Figure 2.3C) demonstrates a C_t profile that is more typical for a chlorophyll concentration profile for this type of water.

(C) Spectrophotometric particulate absorption data were obtained at 31 stations, and spectrophotometry of MeOH and acetone extracts done at 14 stations. Spectra from station 91 are shown in Figure 2.2. The UV-B absorbing mycosporine-like-amino acids (MAA) compounds were present as indicated by the peak in the spectrum below 350nm. Acetone absorbs wavelengths around this region (arrow in Figure 2.2) and therefore is not appropriate for the analysis of MAA compounds.

(D) Too few data were obtained during Leg I to obtain a good description of the horizontal 5m chlorophyll distribution. The horizontal distribution for Leg II is shown in Figure 2.4A. This compares well to the medium resolution SeaWiFS monthly composite of surface chl-*a* in the region (Figure 2.4B). During Leg II, phytoplankton biomass measured for 5m samples in the Elephant Island area was 1.50 +/- 1.07 mg chl-*a* m^{-3} (58 stations). For the same region, SeaWiFS monthly composite gave an estimate (using the SeaWiFS algorithm) of only 0.6 mg chl-*a* m^{-3}. Bio-optical algorithms for either ocean color remote sensing or diffuse attenuation coefficients are different in temperate and polar regions (Mitchell and Holm-Hansen, 1991; Mitchell, 1992; Arrigo *et al*., 1998). For US JGOFS data, Moore *et al*., (1999) have shown that SeaWiFS underpredicts chl-*a* by about 30% compared to *in situ* estimates. Previously, we hypothesized that pigment package effects and a relative lack of detrital and soluble absorption were responsible for the relationships found for the Antarctic Peninsula region (Mitchell and Holm-Hansen, 1991; Mitchell, 1992). It is important to extend our regional understanding of these algorithms and to assess their implications for remote sensing of pigments, diffuse attenuation coefficients and application of optical-based models of primary production. In particular, no detailed optical measurements have been made in the AMLR survey region prior to this year. Bio-optical relationships and parameterizations will be used to improve applications of both ocean color satellite data and models of primary production in the AMLR survey region.

(E) Monthly composite chlorophyll distributions from SeaWiFS images for January and February of the region covered during the synoptic survey (Leg I) are shown as Figure 2.5. A belt of blue water (Water Zone 1A) lies between South America and the Antarctic Peninsula, and high chlorophyll concentrations appear to reach from the Bransfield Strait region to South Georgia. For the Leg I survey area, highest chlorophyll concentrations were indicated along the western shore of South Georgia (note the bloom development during February). High chlorophyll concentrations are also indicated on the southern shores of the South Orkney Islands during January. In this regard, it appears that the two stations south of South Orkney Islands (Leg I) missed this bloom. The greatest density of surface chlorophyll for the Antarctic Peninsular region occurred on the Weddell Sea side, and is probably an ice-edge related bloom.

(F) One of the key parameters obtainable from satellite measurements is the spectral reflectance, or ocean color, which contains information about optically significant constituents of seawater. The AMLR survey region is a complex system with significant internal gradients in forcing and biogeochemical properties. There remains a critical need to generalize bio-optical properties for bio-geographic provinces of this region and their relation to photosynthesis, biomass, carbon and production.

(G) Apparent optical properties of water including the diffuse attenuation coefficient (K) that specifies the rate of light attenuation of the ocean and the reflectance (R) which is the "ocean

color" depend on inherent optical properties (absorption and scattering) of the medium. Water may contain variable amounts of particulates or soluble material, which affect inherent and apparent optical properties (Morel and Prieur, 1977; Smith and Baker, 1978; Morel, 1988; Mitchell and Holm-Hansen, 1991; Arrigo *et al*., 1998). R and K have been shown to correlate well with the phytoplankton pigments biomass (e.g. chl-*a*) because absorption by pigments dominates variability in these properties. Significant correlations have been reported between POC and the particulate beam attenuation in the AMLR region (Villafañe *et al*., 1993), the northeast Atlantic Ocean (Marra, 1995) and the Pacific Ocean (Bishop, 1999). This good correlation will allow us to interpret beam attenuation data in terms of POC distributions and in relation to physical mixing.

2.4 Disposition of the Samples and Data: All data obtained during the cruises have been stored on CD-ROM. After compilation of the final data sets, a copy of all data will be deposited with the AERG office in La Jolla, CA. Copies of any of our data sets are available to all other AMLR investigators upon request.

2.5 Problems and Suggestions: There were several serious shortcomings this year in regard to facilities and equipment needed on the ship to satisfactorily carry out phytoplankton studies for the AMLR program. Lack of funding greatly restricted both the personnel required on board ship to process samples (previous years we have had four compared to only two persons this year) and restricted the number of analyses that could be accomplished. This year, an optical oceanography program required to develop satellite ocean color algorithms in the AMLR region was initiated. Although much data were collected, it is not known how much will be processed due to lack of funds. In this report, we demonstrate the potential usefulness of synoptic satellite images to describe the large-scale distribution of phytoplankton in the AMLR region. As shown here, and published previously, Southern Ocean regional ocean color algorithms are essential for quantitative application of these satellite data sets. This requires a significant *in situ* phytoplankton and bio-optics effort to provide critical data.

2.6 Acknowledgements: We want to express our gratitude and appreciation to the entire complement of the R/V *Yuzhmorgeologiya* for their generous and valuable help during the entire cruise. They not only aided immeasurably in our ability to obtain the desired oceanographic data, but they also made the cruise most enjoyable and rewarding in many ways. We also thank all other AMLR personnel for help and support which was essential to the success of our program. This work was supported in part by NASA SIMBIOS Project awards to B. Greg Mitchell (NAS5-97130 and S-35780-G).

2.7 References:

Arrigo, K.R., Robinson, D.H., Worthen, D.L., Schieber, B. and Lizotte. 1998. Bio-optical properties of the southwestern Ross Sea. *Journal of Geophysical Research* 103(C10): 21683-21695.

Bishop, J.K.B. 1999. Transmissometer of measurement of POC. *Deep-Sea Research I* 46(2): 353-369.

Marra, J. 1995. Primary production in the North Atlantic: measurements, scaling and optical determinants. *Philosophical Transactions of the Royal Society of London, Series B-Biological Sciences* 348:153-160.

Mitchell, B.G. and Holm-Hansen, O. 1991. Bio-optical properties of Antarctic Peninsula waters: differentiation from temperate ocean models. *Deep-Sea Research I* 38(8/9): 1009-1028.

Mitchell, B.G. 1992. Predictive bio-optical relationships for polar oceans and marginal ice zones. *Journal of Marine Systems* 3: 91-105.

Moore, J.K., Abbott, M.R., Richman, J.G., Smith, W.O., Cowles, J.R., Coale, K.H., Gardner, W.D. and Barber, R.T. 1999. SeaWiFS satellite ocean color data from the Southern Ocean. *Geophysical Research Letters* 26(10): 1465-1468.

Morel, A. 1988. Optical modeling of the upper ocean in relation to its biogenous matter content (case I waters). *Journal of Geophysical Research* 93(C9): 10749-10768.

Morel, A. and Prieur, L. 1977. Analysis of variations in ocean color. *Limnology and Oceanography* 22: 709-722.

Smith, R.C. and Baker, K.S. 1978. The bio-optical state of ocean waters and remote sensing. *Limnology and Oceanography* 23: 247-259.

Villafañe, V., Helbling, E.W. and Holm-Hansen, O. 1993. Phytoplankton around Elephant Island, Antarctica: distribution, biomass and composition. *Polar Biology* 13: 183-191.

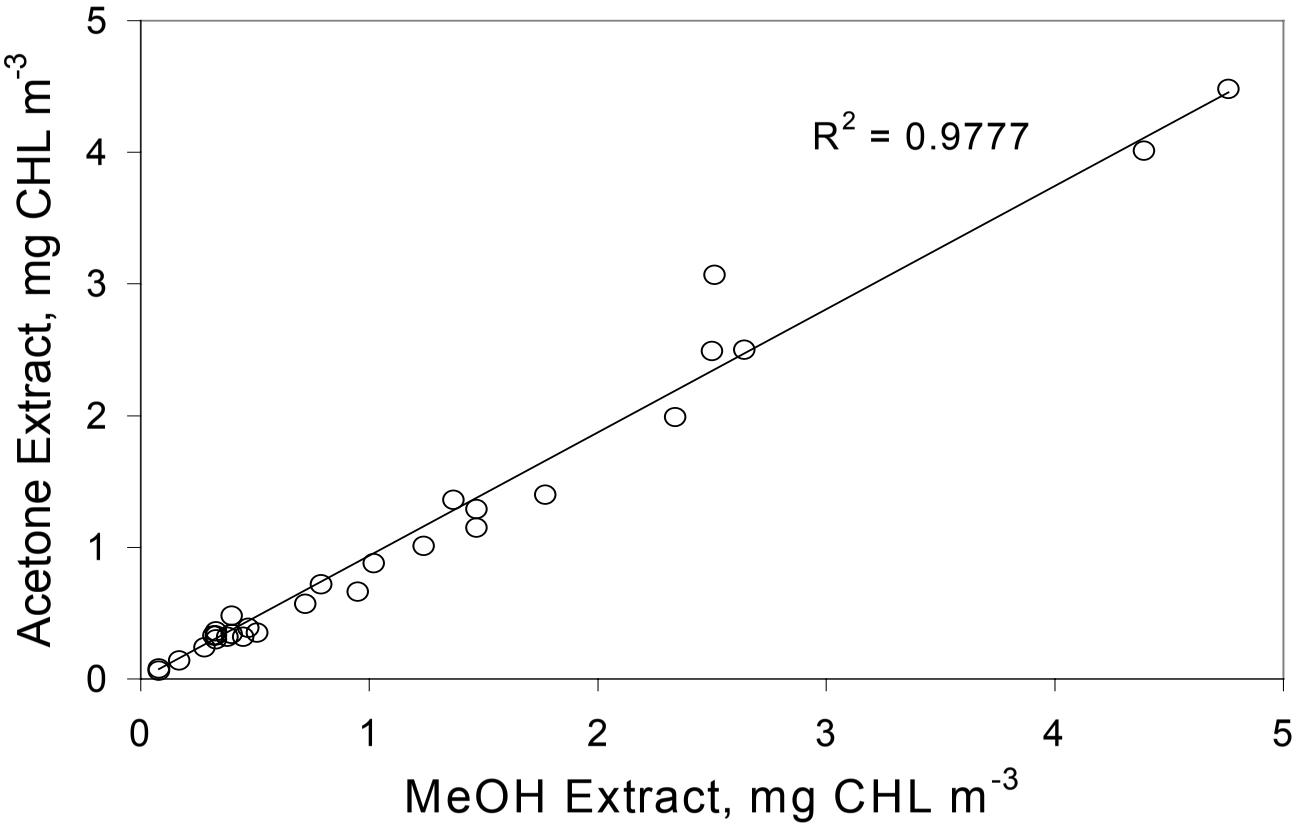

Figure 2.1 Comparison between estimates of chlorophyll concentrations using methanol (MeOH) and 90% acetone. Chl-*a* was extracted using acetone during Leg I, whereas MeOH was used during Leg II (and has been the solvent used for this in all previous years). Additionally, different fluorometers were used for chl-*a* analysis during each leg. Because of differences in methodologies, during Leg I samples for chl-*a* analysis were also frozen in liquid nitrogen until Leg II when MeOH extraction and analysis using the other fluorometer was possible. These data indicate that the two methods were comparable.

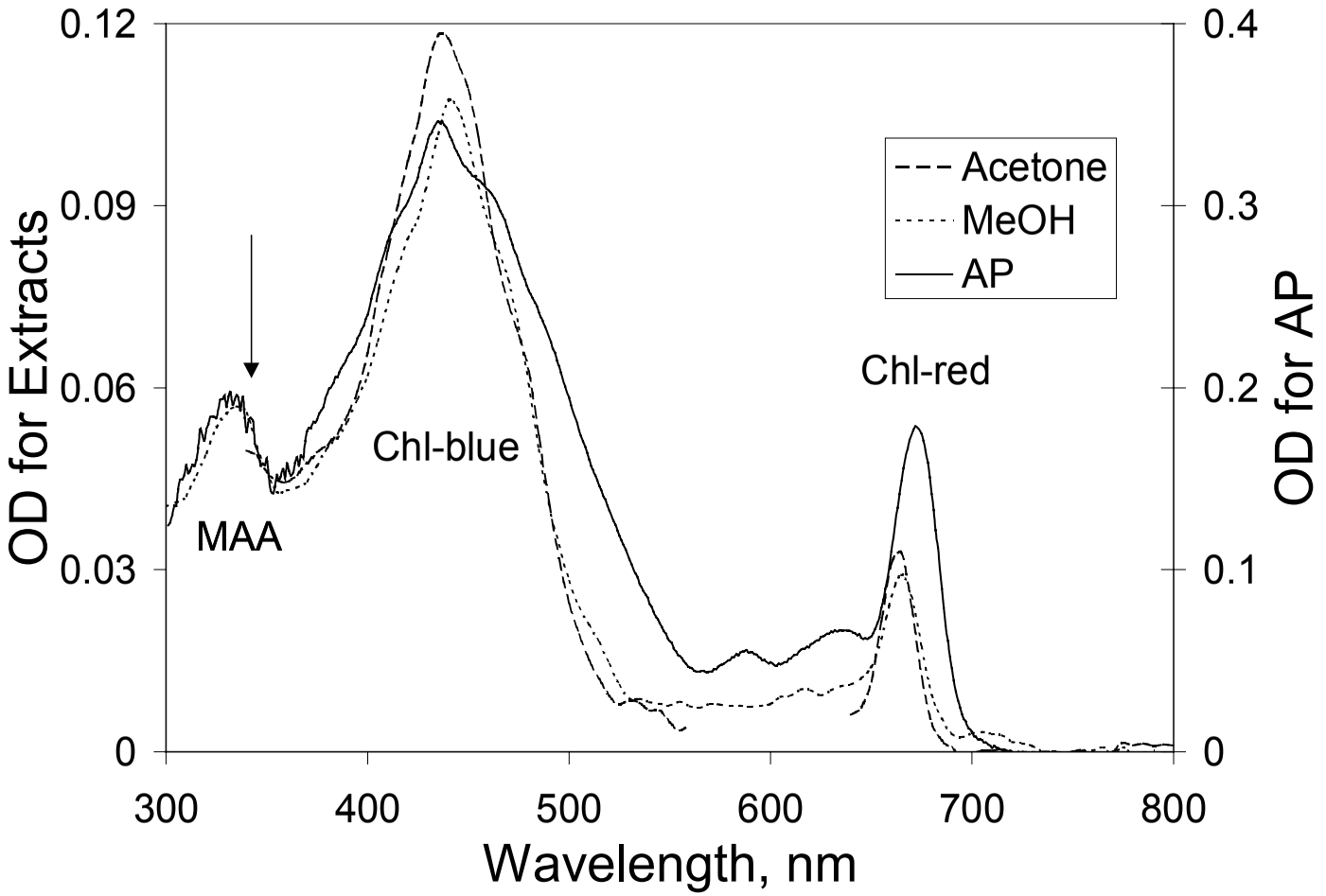

Figure 2.2 Absorption (optical density, OD) spectra for acetone and MeOH extracts and particulates (AP). Chlorophyll absorbs wavelengths in both red (Chl-red) and blue (Chl-blue) wavelengths, and corresponds with the wavelengths used for the two transmissometers (see Figure 2.3). The absorption spectra of UV-B protection MAA compounds is also indicated.

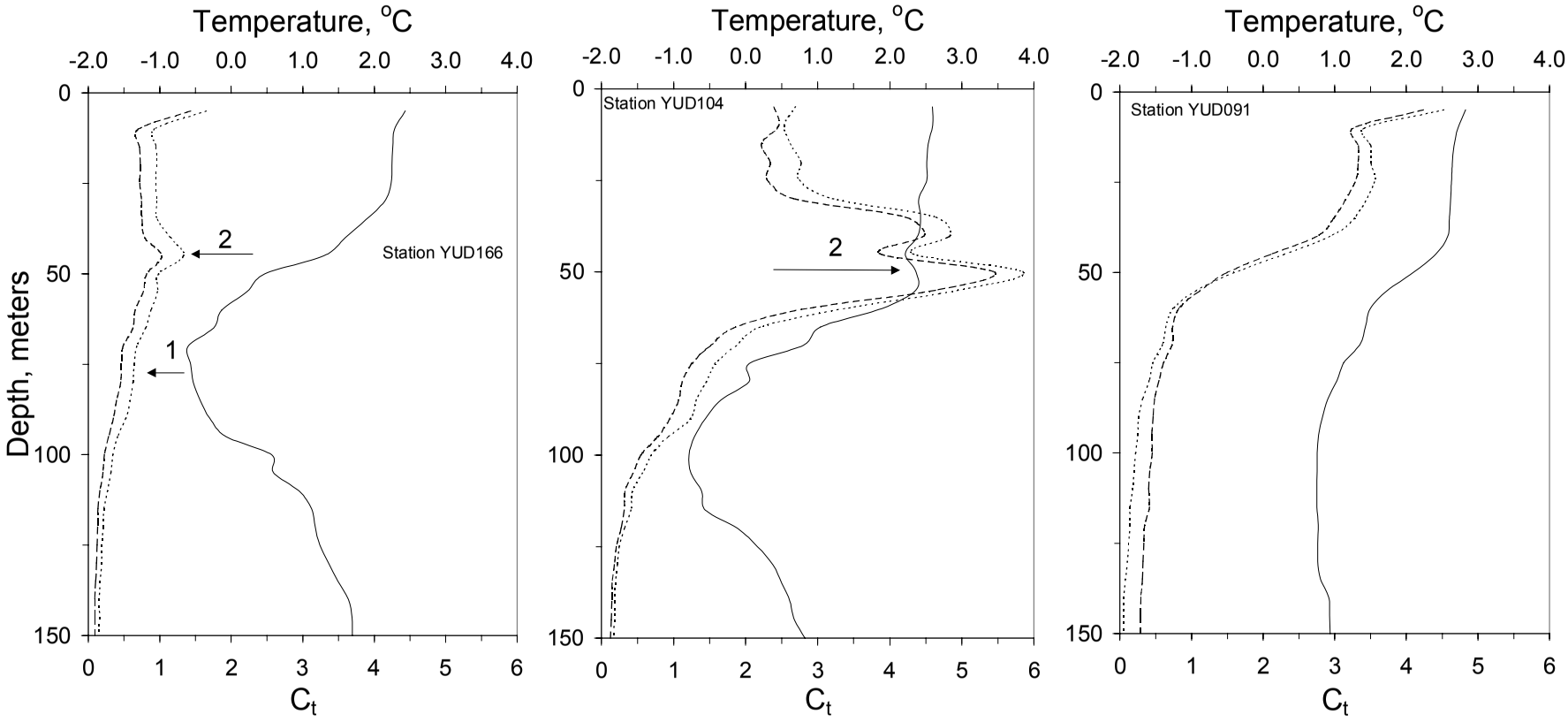

Figure 2.3 Depth profiles for transmissometers (C_t) of 488nm (stippled line) and 660nm (dashed line) and temperature (solid line) from three stations during Leg II. A) Drake Passage (Type1A) water typically has a chl-*a* maximum and a temperature minimum at 75-100m (1), however transmissometer indicated a chl-*a* maximum at the bottom of the upper mixed layer (2). B) Type 1B water differs from 1A water by having a higher chl-*a* concentration in the upper mixed layer. Again, a C_t maximum (2) was observed at the base if the upper mixed layer. C) Bransfield Strait water showing a more classical profile of C_t in the upper mixed layer.

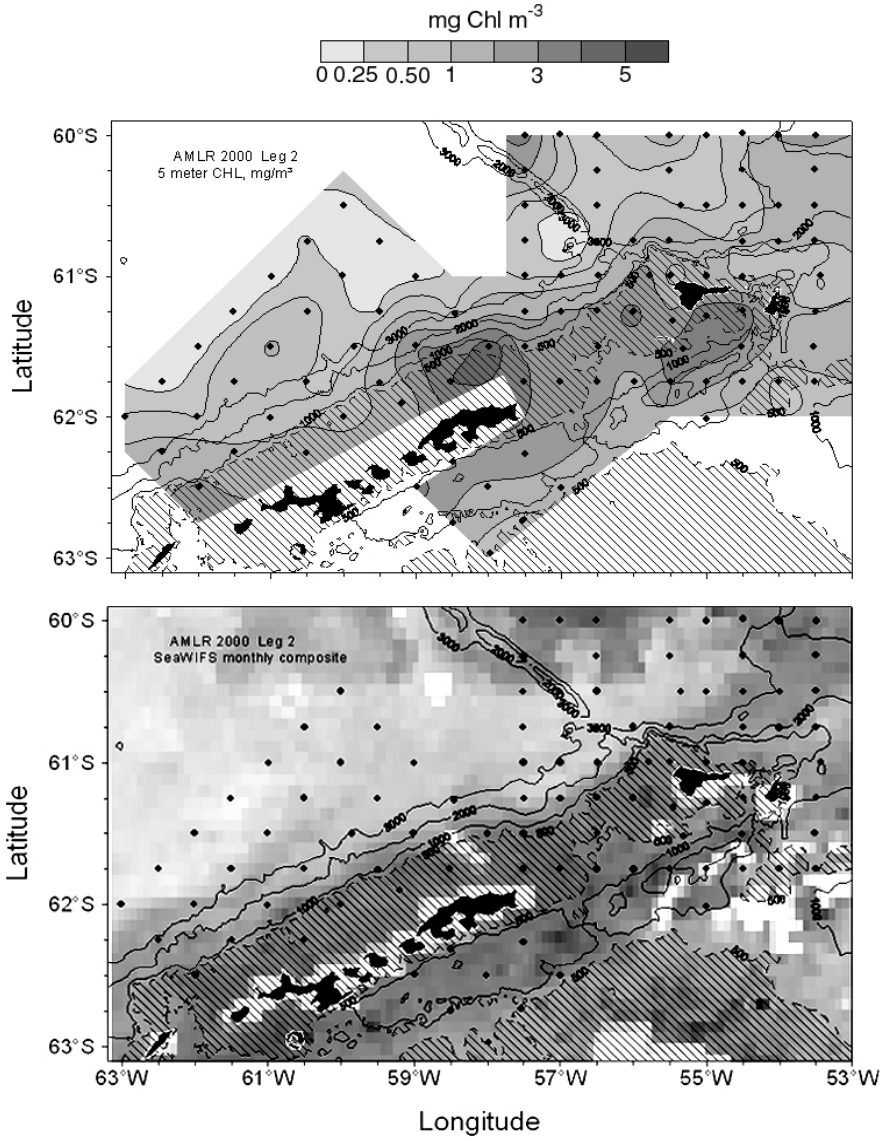

Figure 2.4 Distribution of surface chlorophyll in the AMLR survey area during Leg II. A) Top panel, concentrations estimated from extracted chl-*a* sampled by Niskin bottles at 5m depth. B) Bottom panel, surface concentrations estimated by SeaWiFS algorithms as a February monthly average. Chl-*a* estimated by SeaWiFS algorithm is considered an underestimate (Mitchell and Holm-Hansen, 1991; Moore *et al*., 1999) therefore gray scaling has been adjusted (by eye) to correspond with the range of values from the extractions.

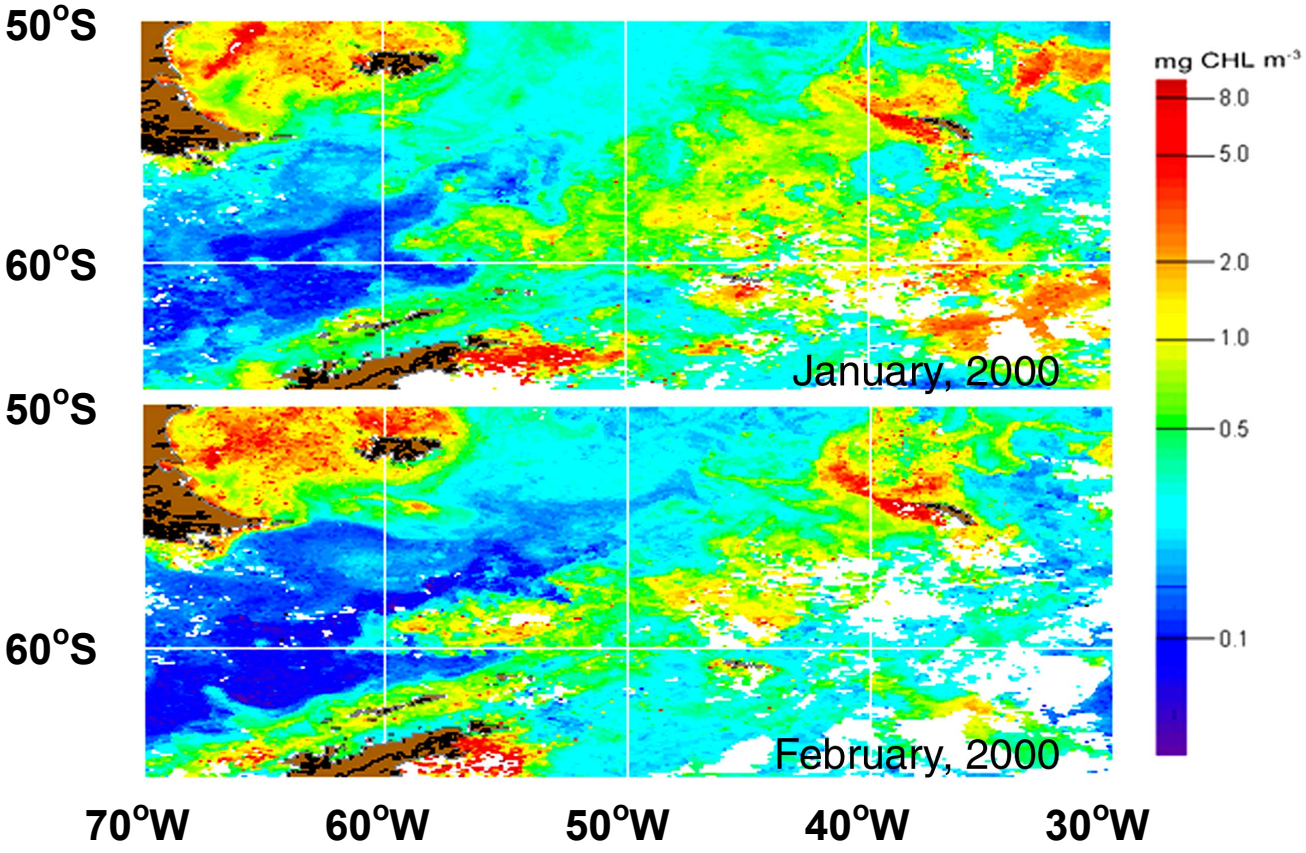

Figure 2.5 January (top panel) and February (bottom panel) of surface chl-*a* distributions (SeaWiFS algorithm) encompassing the area covered during Leg I. Highest chl-*a* (red) occurred on the Weddell Sea side of the Antarctic Peninsula and South Georgia, with moderate (yellow) concentrations spreading as a discontinuous band between them. The lowest concentrations (blue) were found in the Drake Passage between the Antarctic Peninsula and the tip of South America.